THE JOURNAL OF BIOLOGICAL CHEMISTRY VOL. 281, NO. 6, pp. 3439–3451, February 10, 2006


# Vaccinia Virus Uracil DNA Glycosylase Interacts with the A20 Protein to Form a Heterodimeric Processivity Factor for the Viral DNA Polymerase*

Received for publication, October 16, 2005, and in revised form, November 29, 2005 Published, JBC Papers in Press, December 1, 2005, DOI 10.1074/jbc.M511239200

**Eleni S. Stanitsa, Lisa Arps, and Paula Traktman**[1]

*From the Department of Microbiology and Molecular Genetics, Medical College of Wisconsin, Milwaukee, Wisconsin 53226*

**The vaccinia virus E9 protein, the catalytic subunit of the DNA polymerase holoenzyme, is inherently distributive under physiological conditions, although infected cells contain a highly processive form of the enzyme. The viral A20 protein was previously characterized as a stoichiometric component of the processivity factor, and an interaction between A20 and E9 was documented *in vivo*. A20 has been shown to interact with D4, the virally encoded uracil DNA glycosylase (UDG), by yeast-two hybrid and *in vitro* analysis. Here we confirm that UDG and A20 interact *in vivo* and show that temperature-sensitive viruses with lesions in the D4R gene show a profound defect in DNA synthesis at the non-permissive temperature. Moreover, cytoplasmic extracts prepared from these infections lack processive polymerase activity *in vitro*, implicating D4 in the assembly or activity of the processive polymerase. Upon overexpression of 3×FLAG-UDG, A20, and E9 in various combinations, we purified dimeric and trimeric UDG-A20 and UDG-A20-polymerase complexes, respectively. These complexes are stable in 750 mM NaCl and can be further purified by Mono Q chromatography. Notably, the trimeric complex displays robust processive polymerase activity, and the dimeric complex can confer processivity on purified E9. Consistent with previous reports that the catalytic activity of UDG is dispensable for virus replication in tissue culture, we find that the role of UDG role in the polymerase complex is not diminished by mutations targeting residues involved in uracil recognition or excision. Our cumulative data support the conclusion that A20 and UDG form a heterodimeric processivity factor that associates with E9 to comprise the processive polymerase holoenzyme.**

Vaccinia virus, the prototypic orthopoxvirus, shows a significant degree of genetic autonomy from the host cell. Because all stages of the viral life cycle take place in the cytoplasm, vaccinia encodes most, if not all, of the factors involved in the replication of its 192-kb genome. The repertoire of essential replication functions appears to include: E9 (replicative DNA polymerase), A20 (stoichiometric component of the processivity factor), D5 (DNA-independent dNTPase), B1 (Ser/Thr protein kinase), I3 (single strand DNA-binding protein), A22 (Holliday junction resolvase), and D4 (uracil DNA glycosylase, UDG)[2] (Ref. 1, reviewed in Refs. 2 and 3). Other proteins implicated in the process of genome replication or maintenance include A50 (DNA ligase), H6 (topoisomerase), F2 (dUTPase), J2 (thymidine kinase), A48 (thymidylate kinase), and F4/I4 (ribonucleotide reductase) (reviewed in Refs. 2 and 3).

In most cases, a processive DNA polymerase comprises the core of the replication machinery. Processivity, which enables polymerases to replicate long templates rapidly and accurately, is not an intrinsic property of most polymerases but rather is conferred by accessory proteins. Indeed, the vaccinia virus E9 protein, which is the catalytic subunit of the polymerase, is inherently distributive under physiological conditions (4). In our efforts to purify and characterize the vaccinia virus processivity factor, we described the identification of A20 as a stoichiometric component of the processivity factor (5). A20 and E9 were shown to interact *in vivo* by co-immunoprecipitation, and overexpression of A20 and E9 led to a corresponding increase in processive polymerase activity as assayed *in vitro*. Additionally, temperature-sensitive (*ts*) viruses with targeted lesions in A20 had a DNA$^-$ phenotype *in vivo* (6), and extracts prepared from infected cells showed a defect in processive DNA synthesis *in vitro* (6). However, reconstitution of the processive holoenzyme *in vitro* has been elusive, and we have considered the possibility that additional proteins might participate in this process.

Uracil DNA glycosylase enzymes are ubiquitous in prokaryotes and eukaryotes and function as DNA repair enzymes by initiating the base excision repair pathway. They scan DNA and, upon encountering a dUMP residue generated by dUTP misincorporation or dCMP deamination, catalyze the excision of the uracil moiety. The vaccinia virus D4R gene, which encodes the viral UDG, is essential for replication in tissue culture, although the catalytic activity of the protein is dispensable (7). A role for the D4 protein (UDG) in DNA replication emerged from early studies of a *ts* mutant derived from the Dales collection (*ts*4149, now renamed D*ts*30) (8, 9). This *ts*D4 mutant showed a strong DNA$^-$ phenotype when infections were performed at the non-permissive temperature. In contrast, ongoing DNA replication appeared to be spared if D*ts*30 infections were initiated at the permissive temperature and shifted to the non-permissive temperature at 6 hpi (10). It was therefore hypothesized that D4 might be a component of a multiprotein replication complex that would remain stable and functional if assembled at the permissive temperature. Support for this hypothesis emerged later with the observation that UDG shows a strong interaction with A20 in yeast two-hybrid analyses and *in vitro* co-immunoprecipitation experiments (11, 12).

The interaction of UDG with A20, and its apparent role in DNA replication, suggested that it might participate in the assembly of a processive polymerase holoenzyme. We therefore undertook further analysis of the role of UDG *in vivo*, its interaction with A20, and its contribution to polymerase function. These studies were aided by the availability of two *ts* mutants with lesions in the D4R gene, by our con-

* This work was supported by National Institutes of Health Grant R01-AI-21758 (to P. T.). The costs of publication of this article were defrayed in part by the payment of page charges. This article must therefore be hereby marked "*advertisement*" in accordance with 18 U.S.C. Section 1734 solely to indicate this fact.

[1] To whom correspondence should be addressed: Dept. of Microbiology and Molecular Genetics, Medical College of Wisconsin, 8701 Watertown Plank Road, BSB-273, Milwaukee, WI 53226. Tel.: 414-456-8253; Fax: 414-456-6535; E-mail: ptrakt@mcw.edu.

[2] The abbreviations used are: UDG, uracil DNA glycosylase; araC, arabinofuranosylcytosine; *ts*, temperature-sensitive; ORF, open reading frame; wt, wild type; TBS, Tris-buffered saline; pol, polymerase; IVTT, *in vitro* transcription-translation; m.o.i., multiplicity of infection; RFII, replicative form II; hpi, hours post-infection; PCNA, proliferating cell nuclear antigen; CMV, cytomegalovirus.

struction of a recombinant virus encoding epitope-tagged UDG at the endogenous locus, and by the overexpression and purification of epitope-tagged UDG alone or in the context of overexpressed A20 and/or E9. In sum, our data support the conclusion that A20 and UDG, along with E9, are necessary and sufficient components of the processive polymerase holoenzyme.

## EXPERIMENTAL PROCEDURES

### Materials, Cells, Viruses, and DNA Plasmids

African green monkey kidney BSC40 cells and human TK$^-$ 143 cells were cultured in Dulbecco's modified Eagle's medium containing 5% fetal calf serum (Invitrogen). The recombinant vaccinia virus vTF7.5 was a gift from B. Moss (National Institutes of Health, Bethesda, MD); the temperature-sensitive viruses D*ts*27 and D*ts*30, from the Dales collection, were provided by R. Condit (University of Florida, Gainesville, FL). The pTM1–3×FLAG plasmid, which enables the T7 RNA polymerase-mediated expression of N-terminally 3×FLAG-tagged proteins, has been previously described (13). Viral stocks were prepared by ultracentrifugation of cytoplasmic lysates through 36% sucrose; titration was performed on confluent monolayers of BSC40 cells, which were stained with crystal violet at 48 hpi except where indicated. Arabinofuranosylcytosine (araC), pancreatic RNase, α-FLAG M2 monoclonal antibody, α-FLAG-agarose beads, and 3×FLAG peptide were purchased from Sigma. Restriction endonucleases, T4 DNA ligase, Taq polymerase, and calf intestinal phosphatase were purchased from Roche Applied Science, whereas Geneticin (G418 sulfate) was purchased from Invitrogen. Protein molecular weight markers, $^{14}$C-labeled, were purchased from Amersham Biosciences, and DNA molecular weight standards were purchased from Invitrogen. [$^{32}$P]Orthophosphate and [$^{35}$S]methionine were purchased from PerkinElmer Life Sciences and Analytical Sciences, Inc. (Boston, MA). DNA oligonucleotides were synthesized by IDT (Coralville, IA). Protein standards were purchased from Invitrogen, and *Escherichia coli* SSB was acquired from Stratagene (La Jolla, CA).

### Singly Primed M13 DNA Replication Assay

A primed M13 template was prepared by annealing a 24-mer primer (5′-CGCCAGGGTTTTCCCAGTCACGAC-3′) to M13mp10 single-stranded DNA at a molar ratio of 20:1 (5). Extracts of infected cells or eluates retrieved after affinity chromatography on agarose beads containing immobilized α-FLAG antibody were assayed in 25-μl reactions containing 10 mM Tris-HCl (pH 7.4), 40 ng/μl bovine serum albumin, 8% glycerol, 0.1 mM EDTA, 5 mM dithiothreitol, 8 mM $MgCl_2$, 25 fmol of singly primed M13mp10 single-stranded DNA, 750 ng of *E. coli* SSB (10 pmol of tetramer), 60 μM each of dCTP, dGTP, and dATP, and 20 μM α-[$^{32}$P]TTP (2400 cpm/pmol). Preparations containing purified vaccinia virus DNA polymerase (E9 protein, purified as described in Ref. 14) were added where indicated. As previously described, the 20-min primer extension reaction was initiated by adding dATP and [$^{32}$P]TTP after a 3-min preincubation that was performed in the presence of only dCTP and dGTP (5). Reactions were quenched by the addition of an equal volume of 1% SDS-40 mM EDTA and resolved on 0.8% agarose gels containing 0.125 μg/ml ethidium bromide. Gels were cast and run in Tris borate-EDTA buffer; radiolabeled products were visualized by autoradiography and quantitated on a Storm PhosphorImager (Amersham Biosciences). The data were quantitated using ImageQuaNT software (Amersham Biosciences) and plotted using SigmaPlot (SSPS, Chicago, IL) software.

### Computer Analysis

Autoradiographic films were scanned and adjusted with Adobe Photoshop (Adobe Systems, Inc.) or Canvas 8.0 (Deneba Systems, Miami, FL.) software. Figures were labeled with Canvas 8.0.

### Construction of Recombinant Vaccinia Viruses

*vvfUDG: Recombinant Virus in Which 3×FLAG-UDG Is Expressed from the Endogenous D4R Locus*—For preparation of pUCneo-D3–3XFLAG-D4, a cassette comprised of the 3′ 300 bp of D3R, 66 bp encoding the 3×FLAG epitope, and the 5′ 300 bp of the D4R ORF was prepared by overlap PCR. One of the initial PCR reactions was performed with an upstream primer (A: 5′-CGGGATCCTATTCGTACAGGTACCTC-3′), which introduces a BamHI site (underlined) upstream of sequences derived from the 3′ region of the D3R gene and a downstream primer (5′-GATGTCATGATCTTTATAATCACCGTCATGGTCTTTGTAGTCCATTATATCAAATTAGATAC-3′), which contains 43 nucleotides from the 3×FLAG sequence (underlined) and anneals to the terminal 19 bp of D3R. A second reaction was performed with an upstream primer (5′-TATAAAGATCATGACATCGATTACAAGGATGACGATGACAAGAATTCAGTGACTGTATCA-3′) that also carries sequences derived from the 3×FLAG sequence (underlined) and anneals to the 5′ region of the D4R sequence, and a downstream primer (B: 5′-CGGGATCCCTTTATAATCAATTACTCCGG-3′) that introduces a unique BamHI site (underlined) downstream of sequences located within the D4R gene. The products derived from these two reactions overlap by 17 bp and were used together as the templates for a second round of PCR performed with the outside primers A and B. The 730-bp product generated in this reaction was digested with BamHI and ligated into pUCneo DNA that had been previously digested with BamHI and treated with calf intestinal phosphatase. This plasmid also encodes the *NEO* gene under the regulation of a constitutive viral promoter (15). For generation of vvfUDG, the overall strategy was to replace the endogenous D4 locus with one encoding a 3XFLAG-tagged allele; this was accomplished using the plasmid described above and wt virus. Generation of the virus was achieved by transient dominant selection as described (6, 16, 17).

*vT7fUDG: Recombinant Virus Enabling T7 Polymerase-mediated Overexpression of 3x-fUDG*—For preparation of pTM-3XFLAG-UDG, the D4R ORF was amplified from genomic DNA using an upstream primer (UpD4: 5′-GGAAGTCCAT**ATG**AATTCAGTGACTGT-3′), which introduced an NdeI site (underlined) at the translational initiation codon (bold), and a downstream primer (DownD4: 5′-CGGGATCC**TTA**ATAAATAAACCCTTG-3′), which introduced a unique BamHI site (underlined) downstream of the translational termination codon (bold). The PCR product was digested with NdeI and BamHI and ligated into pTM-3×FLAG vector DNA that had been similarly digested and treated with calf intestinal phosphatase. For generation of vT7fUDG, the overall strategy was to place the T7-driven 3XFLAG-UDG cassette within the non-essential TK locus of wt virus. Generation of this virus was achieved by selection of TK$^-$ viruses after transfecting wt-infected cells with the plasmid described above; the strategy followed has been previously described (13, 14, 18).

*vvT7fUDG⃠: Recombinant Virus Enabling T7 Polymerase-mediated Overexpression of 3×-FLAG-tagged Catalytically Null UDG*—For generation of pTM-3XfUDG⃠, two rounds of overlap PCR were used to introduce two mutations into the D4R ORF that render the UDG catalytically inactive (Gly$^{202}$ → Ala and Ala$^{542}$ → Thr). First, PCR was performed using the previously described upstream primer (UpD4), which places an NdeI site at the D4R initiation codon and a downstream primer (Down202A: 5′-ATACGGATTTATACCACACACAC-3′) that

encodes the $Cys^{202} \rightarrow Thr$ substitution (underlined). A second PCR was performed using an upstream primer (Up202: 5′-GTGGTATAAATC-CGTATCCGAAA-3′) that encodes the $Gly^{202} \rightarrow Ala$ (underlined) and the previously described downstream primer (DownD4) that places a BamHI site downstream of the D4R termination codon. The 225-bp and 469-bp products generated in these two PCR reactions overlap by 17 bp and were used together as the template for a second round of PCR, which was performed with the outside primers UpD4 and DownD4. This 675-bp product represented a variant of the complete D4R ORF containing an internal $Gly^{202} \rightarrow Ala$ substitution. This product was used as the template for a second round of overlap PCR designed to introduce the $Ala^{542} \rightarrow Thr$ mutation. The primer sets used for the introduction of this mutation were 1: UpD4 and Down542 (5′-CCGCTGGAA-GATATCCCACTATG-3′; mutation underlined) and 2: Up524 (5′-GGGATATCTTCCAGCGGCTAGAG-3′; mutation underlined) with DownD4. The resulting products, which were of 130 and 562 bp in length and overlapped by 17 bp, were used together as the template for a final round of PCR performed with the outside primers UpD4 and DownD4. The final 675-bp product represented a variant of the complete D4R ORF containing both the $Gly^{202} \rightarrow Ala$ and $Cys^{542} \rightarrow Thr$ mutations. This product was digested with NdeI and BamH1 and cloned into pTM3×FLAG as described above. Isolation of vT7fUDG⊘ from cells infected with wt virus and transfected with pTM3xfUDG⊘ was performed as described above.

*pTM3×FLAG-fUDG⊗: Plasmid Enabling T7 Polymerase-mediated Overexpression of 3×-FLAG-tagged ($Tyr^{70}$-$Phe^{79}$-$Asn^{120} \rightarrow Ala$) Mutant UDG*—For generation of pTM-3XfUDG⊗, three rounds of overlap PCR were used to introduce three mutations into the D4R ORF that render the UDG unable to recognize and bind uracil ($Tyr^{70}$-$Phe^{79}$-$Asn^{120} \rightarrow Ala$). First, PCR was performed using the previously described upstream primer (UpD4), which places an NdeI site at the D4R initiation codon and a downstream primer (DownT70A: 5′-GTTC-CATCTTTCGGAGCCGGATCTA-3′) that encodes the substitution (underlined). A second PCR was performed using an upstream primer (UpY70A: 5′-TAGATCCGGCTCCGAAAGATGGAAC-3′) and the previously described downstream primer (DownD4) that places a BamHI site downstream of the D4R termination codon. The 230- and 445-bp products generated in these two PCR reactions overlap by 17 bp and were used together as the template for a second round of PCR, which was performed with the outside primers UpD4 and DownD4. This 675-bp product represented a variant of the complete D4R ORF containing an internal substitution that leads to the $Tyr^{70} \rightarrow Ala$ mutation. This product was used as the template for a second round of overlap PCR designed to introduce the $Phe^{79} \rightarrow Ala$ mutation. The primer sets used for the introduction of this mutation were 1: UpD4 and DownF79A (5′-AATTTGGTGATTCGGCCGGTACAC-3′; mutation underlined) and 2: UpF79A (5′-GTGTACCGGCCGAATCACCAAA-TT-3′; mutation underlined) with DownD4. The resulting products, which were of 250 and 430 bp in length and overlapped by 17 bp, were used together as the template for the overlap PCR performed with the outside primers UpD4 and DownD4. The final 675-bp product represented a variant of the complete D4R ORF containing both the Y70A and F79A mutations. The primer sets used to introduce the N120A mutation were 1: UpD4 and Down N120A (5′-CAACTTAAGTAATA-AGCCCAGGGTA-3′; mutation underlined) and 2: DownD4 with UpN120A (5′-TACCCTGGGCTTATTACTTAAGTTG-3′; mutation underlined). The resulting products (375 and 300 bp, respectively) were used together as the template for the final round PCR using the two outside primers UpD4 and DownD4. This product was digested with NdeI and BamH1 and cloned into pTM3×FLAG as described above.

### Overexpression and Purification of fUDG, A20, and DNA Polymerase (E9)

Overexpression of fUDG, A20, and E9, singly and in combination, was achieved by co-infecting confluent monolayers of BSC40 cells with vTF7.5, which constitutively expresses the T7 polymerase, and vT7fUDG, vT7A20, and/or vT7pol (each at m.o.i. 2) as appropriate (5, 14). Infections were initiated at 37 °C and shifted to 31.5 °C at 4 hpi to increase the yield of soluble protein. Cells were harvested at 24 hpi and solubilized in FLAG-lysis buffer (50 mM Tris-HCl (pH 7.4), 150 mM NaCl, 1 mM EDTA, 1% Triton X-100; 1 ml/$10^7$ cells). Lysates were clarified by low speed centrifugation (800 × *g*, 10 min); lysates that were assayed directly for processive polymerase activity were subjected to further clarification by sedimentation at 16,000 × *g* for 20 min. Affinity purification of fUDG was performed on agarose beads containing immobilized α-FLAG antibody (~20 μl of packed beads/$10^7$ cells). Non-specifically bound proteins were removed by 3 washes with FLAG-TBS buffer (fTBS, 50 mM Tris-HCl (pH 7.4), 150 mM NaCl). Where indicated, the beads were incubated with FLAG-TBS buffer containing increasing concentrations of NaCl, and finally fUDG and any associated proteins were eluted by the subsequent application of 3×FLAG peptide (150 ng/μl). Aliquots were resolved on 12% SDS-PAGE, and proteins were either visualized by silver-staining or transferred to nitrocellulose and subjected to immunoblot analysis as indicated.

In some cases, the fUDG-A20-pol complex was further purified from excess free fUDG by anion exchange chromatography. Approximately 25 μg of the fUDG-A20-pol protein complex purified on α-FLAG beads as described above was diluted in buffer A (50 mM Tris-HCl, 150 mM NaCl, 1 mM dithiothreitol, 1 mM EDTA, and 10% glycerol) before being applied to a 1-ml Mono Q HR 5/5 anion exchange column (Amersham Biosciences) equilibrated in the same buffer. The column was washed with buffer A and then developed with a 10-ml linear gradient of 150–1000 mM NaCl. The trimeric complex was retrieved in three fractions containing 550–590 mM NaCl. Aliquots were stored in 15% glycerol at −20 °C.

### Analysis of UDG and A20 by in Vitro Transcription-Translation Analysis

The plasmids pTM-3xfUDG, pTM-A20 (5, 6), pTM-Pol (14), pTM-3xfUDG*ts*27, pTM-3xfUDG*ts*30, pTM-A20*ts*5ER, or pTM-A20*ts*6 (6) (1 μg each) were used in IVTT reactions (TNT, Promega, Madison, WI) in the presence of 10 mCi/ml [$^{35}$S]methionine (Redivue, Amersham Biosciences). To construct the plasmids pTM-3xfUDG*ts*27 and pTM-3xfUDG*ts*30, the previously described UpD4 and DownD4 primers were used to amplify the D4R ORFs from the genomes of D*ts*27 and D*ts*30; the products were digested with NdeI and BamH1 and ligated to similarly digested pTM3×FLAG DNA. The products of IVTT reactions were either analyzed directly or diluted in FLAG-lysis buffer and subjected to immunoprecipitation analysis with α-FLAG-agarose beads. IVTT products and immunoprecipitates were fractionated on 12% SDS-PAGE and visualized by autoradiography or by quantitative PhosphorImager analysis.

### Immunoblot Analysis

Cell extracts were fractionated by SDS-PAGE, and the proteins were transferred electrophoretically to nitrocellulose membrane (Schleicher & Schuell, Keene, NH) in Tris-glycine buffer (25 mM Tris, 192 mM glycine, 20% methanol). Blots were incubated with α-FLAG M2 according to the instructions of the manufacturer (Sigma) or with α-A20 (5) or α-D5 sera (1:500 dilution) and subsequently incubated with horseradish peroxidase-conjugated goat anti-rabbit immunoglobulin G (1:20,000)

(Bio-Rad). Immunoreactive proteins were visualized by chemiluminescence using Pierce Super Signal reagents.

#### Immunoprecipitation Analysis of Metabolically Labeled Cell Extracts

To monitor the temporal expression of fUDG, confluent monolayers of BSC40 cells were infected with vvfUDG (m.o.i. 15); controls were left uninfected or infected with *wt* virus. At the times indicated, cells were rinsed with Dulbecco's modified Eagle's medium lacking methionine and labeled for 45 min with Dulbecco's modified Eagle's medium lacking methionine containing [$^{35}$S]methionine at 100 $\mu$Ci/ml. Cells were rinsed with ice-cold phosphate-buffered saline and lysed by the addition of 1× phospholysis buffer lacking sodium deoxycolate (0.1 M $NaPO_4$ (pH 7.4), 0.1 M NaCl, 1% Triton X-100, 0.1% SDS, 1 ml/3 × $10^6$ cells). Clarified lysates were subjected to immunoprecipitation with the monoclonal $\alpha$-FLAG M2 antibody; immunoprecipitates were retrieved on protein A-Sepharose beads, resolved on 12% SDS-PAGE, and visualized by autoradiography and/or immunoblot analysis.

#### Marker Rescue

35-mm dishes of BSC40 cells were infected with D*ts*27 or D*ts*30 at an m.o.i. of 0.03 and incubated at 31.5 °C. At 4 hpi, cells were transfected with 3.5 $\mu$g of linearized plasmid DNA preparations containing no insert, the D4R ORF, or the genomic HindIII D fragment. At 7 hpi, cultures were shifted to 39.7 °C; cells were harvested at 48 hpi, and the yield of temperature-insensitive virus was determined by titration at 39.7 °C.

#### Determination of 24-h Viral Yield

Confluent 35 mm-diameter dishes of BSC40 cells were infected with vfUDG, D*ts*27, or D*ts*30 (m.o.i. 2) and incubated at 31.5 or 39.7 °C. At 24 hpi cells were harvested and resuspended in 1 mM Tris, pH 9. Viral yields were determined by titration at 31.5 °C.

#### Analysis of Viral DNA Accumulation by Southern Dot Blot Hybridization

35-mm diameter dishes of BSC40 cells were infected with either vfUDG, D*ts*27, or D*ts*30 (m.o.i. of 2) and were maintained at 31.5 or 39.7 °C. At 3, 6, 9, and 24 hpi, cells were harvested, washed, and resuspended in loading buffer (10× SSC (1× is 0.15 M NaCl, 0.015 M sodium citrate)/1 M ammonium acetate). 25-$\mu$l aliquots of each sample were applied to a Zeta probe membrane using a Bio-Dot microfiltration apparatus (both from Bio-Rad). Samples were denatured (with 1.5 M NaCl and 0.5 M NaOH) and washed twice *in situ* (with 10×SSC). The membrane was hybridized to a $^{32}$P-labeled probe representing the genomic HindIII E and F fragments. Data were analyzed by PhosphorImager analysis.

#### E9 DNA pol Purification

Purification of the E9 protein, the catalytic polymerase, was described previously using the hybrid vaccinia T7 system (14). In brief, overexpression of DNA polymerase was achieved by co-infecting BSC40 cells with vTF7.5 and vT7pol (each at m.o.i. = 2). Infections were initiated at 37 °C and shifted to 31.5 °C at 4 hpi to increase the yield of soluble protein. Cells were harvested at 24 hpi, and clarified cytoplasmic lysates were fractionated sequentially on DEAE-cellulose, phosphocellulose, hydroxyapatite, and heparin-agarose. Enzymatic activity of the purified DNA polymerase was assayed using an activated salmon sperm DNA template; protein concentration was determined by digital evaluation of silver-stained gels.

## RESULTS

Several lines of evidence have confirmed that the vaccinia virus A20 protein plays an essential role as a stoichiometric component of the processive form of the viral DNA polymerase (5, 6). However, confirmation that A20 is the *bona fide* processivity factor has been hampered by our inability to express and purify soluble A20 for the purpose of reconstituting the processive polymerase holoenzyme *in vitro*. We reasoned that A20 might require an additional protein partner for solubility; indeed, a strong interaction between A20 and D4, the viral uracil DNA glycosylase (UDG), has been demonstrated through the use of yeast two-hybrid and glutathione *S*-transferase pull-down analyses (11, 12). The hypothesis underlying the work described herein, therefore, was that UDG might in fact play a role in the assembly of the processive DNA polymerase complex.

#### Characterization of Two Temperature-sensitive Vaccinia Viruses with Lesions in the D4 ORF

##### Mapping of the Lesions by Marker Rescue and DNA Sequencing

Two temperature-sensitive viral mutants within the re-evaluated Dales collection have been thought to contain lesions within the D4R ORF, which encodes the viral UDG. D*ts*30 (*ts*4149) was studied previously, and the D4R gene was shown to contain a $G^{535} \rightarrow A$ transition leading to $Gly^{179} \rightarrow Arg$ substitution (10). Pulse field gel electrophoresis and Southern dot blot analyses indicated that this virus exhibited a severe $DNA^-$ phenotype at the non-permissive temperature, synthesizing ~1% of the levels of DNA made by *wt* virus under comparable conditions (8, 10). D*ts*27 (*ts*3578), however, had not been studied. We determined the DNA sequence of the D4 genes of the wt IHD-W strain and that of D*ts*27. The D*ts*27 ORF contains a $C^{328} \rightarrow T$ transition, which is predicted to generate a $Leu^{110} \rightarrow Phe$ substitution.

To confirm that the D4 lesions were indeed responsible for the temperature sensitivity of both of these mutants, we performed marker rescue experiments. Vectors encoding the HindIII D fragment or a *wt* D4 allele were tested for their ability to generate temperature-insensitive progeny upon recombination into the D*ts*27 and D*ts*30 genomes. The yield of temperature-insensitive progeny obtained after transfection with either of these plasmids was ~100-fold greater than after transfection of an empty vector (not shown).

##### Phenotypic Analysis of Dts30 and Dts27

*Virus Production and Plaque Formation*—The temperature sensitivity of these viruses was assessed by performing single-step yield experiments and plaque assays at both the permissive (31.5 °C) and non-permissive (39.7 °C) temperatures. BCS40 cells were infected with the *ts* mutants or *wt* virus (WR strain) at an m.o.i. of 2 and the 24 h viral yield was quantitated. D*ts*27-infected cultures produced nearly *wt* levels of virus at 31.5 °C but exhibited a tight temperature-sensitive phenotype, producing ~1000-fold less virus at 39.7 °C than at 31.5 °C. The yield obtained from cells infected with D*ts*30 at 31.5 °C was ~5-fold lower than that obtained from *wt* infections, and a further reduction of ~100-fold was obtained from cells infected at 39.7 °C (Fig. 1*A*). Similar results were obtained when infections were performed at an m.o.i. of 15 (not shown). Plaque assays were also performed with these viruses (Fig. 1*B*). As expected, *wt* virus produced plaques at both temperatures; note that the IHD strain produces plaques with comets due to high levels of extracellular enveloped virus release (19). D*ts*27 produced reasonably sized plaques at the low temperature but virtually no macroscopic plaques at the high temperature. D*ts*30 produced small plaques at 31.5 °C and miniscule plaques at 39.5 °C, consistent with the 24-h yield data presented in Fig. 1*A*.

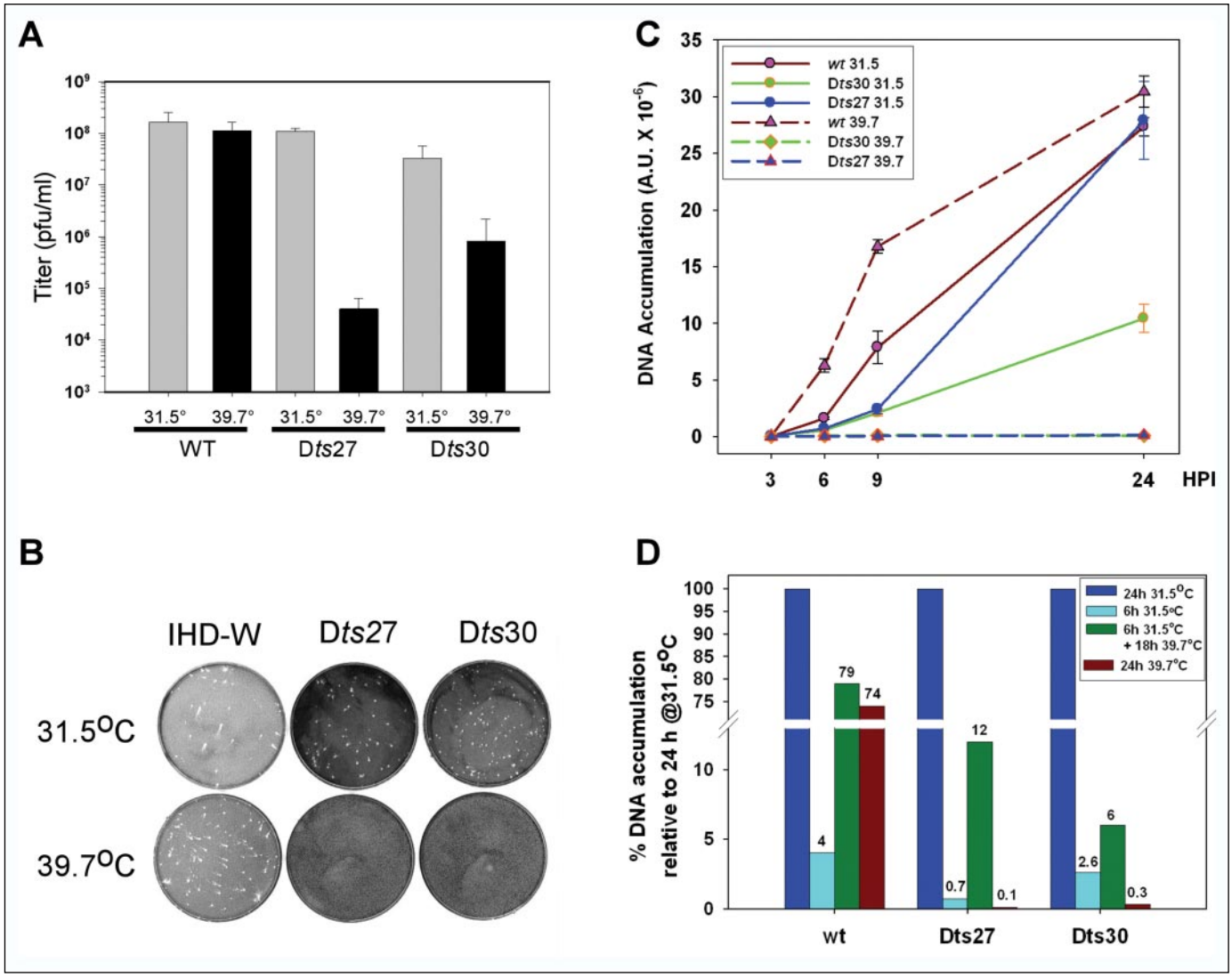


FIGURE 1. **Phenotypic analysis of two temperature-sensitive mutants with defects in the D4R gene.** *A*, quantitation of viral yield produced from single rounds of infection. Confluent monolayers of BSC40 cells were infected with D*ts*27, D*ts*30, and *wt* virus (IHD-W strain) (m.o.i. 2) and incubated at 31.5 or 39.7 °C for 24 h. Cells were harvested and the viral yield was determined by plaque assays performed at 31.5 °C. *B*, D*ts*27 and D*ts*30 do not form plaques at the non-permissive temperature. BSC40 cells were infected with equal numbers of plaque-forming units of *wt* virus, D*ts*27 or D*ts*30 and maintained at 31.5 or 39.7 °C for 48 h prior to being stained. *C*, DNA replication is abrogated in non-permissive D*ts*27 and D*ts*30 infections. BSC40 cells were infected with either *wt* virus, D*ts*27, or D*ts*30 and maintained at 31.5 °C or 39.7 °C. At 3, 6, 9, and 24 hpi cells were harvested and the accumulation of viral DNA was monitored by dot blot hybridization; a graphic representation of the profile of DNA accumulation is shown. *D*, impact of temperature-shift protocols on the DNA$^-$ phenotype observed during D*ts*27 and D*ts*30 infections. Cells were infected with *wt* virus, D*ts*27 or D*ts*30 for 24 h at 31.5 °C (*blue bars*), 6 h at 31.5 °C (*cyan bars*), 6 h at 31.5 °C followed by 18 h at 39.7 °C (*green bars*), or 24 h at 39.7 °C (*maroon bars*). The levels of accumulated viral DNA were determined by dot blot hybridization; for each virus, the data were normalized to the amount of DNA accumulated after 24 h at 31.5 °C. The percent values are shown *above the bars*.

*DNA Replication Is Abrogated at the Non-permissive Temperature*—Based on previous data, we presumed that the temperature sensitivity of these viruses reflected an impairment of viral DNA replication (10). Therefore, we quantitated the accumulation of viral DNA during 31.5 °C and 39.7 °C infections performed with *wt* virus, D*ts*27 or D*ts*30. The results of dot blot hybridization analyses are shown graphically in Fig. 1*C*. When cells were infected with *wt* virus, accumulation of viral DNA was similar at both temperatures, although the rate of accumulation was slightly faster at the higher temperature. During permissive D*ts*27 infections, viral DNA accumulated to levels comparable to those seen during the *wt* infections, although the rate of accumulation was slow until 9 hpi. During permissive D*ts*30 infections, however, the levels of DNA that accumulated were <50% of those seen during *wt* infections. Most importantly, the accumulation of viral DNA was abrogated during non-permissive infections performed with either *ts* mutant. These data provide compelling evidence that lesions in the D4R gene severely compromise DNA replication, supporting an essential role for the vaccinia virus UDG in DNA synthesis.

As another test of the direct role of UDG in viral DNA synthesis, we performed a series of shift-up experiments (Fig. 1*D*). An early report on D*ts*30 suggested that viral DNA synthesis could progress at the non-permissive temperature if the first 6 h were performed at the permissive temperature (10); these data suggested that synthesis of UDG at the non-permissive temperature might impair its folding or assembly into a productive replication complex. We therefore infected cells with either wt virus, D*ts*27, or D*ts*30 and monitored the levels of viral DNA that had accumulated after: 24 h at 31.5 °C (*blue bars*); 6 h at 31.5 °C (*cyan bars*), 6 h at 31.5 °C followed by 18 h at 39.7 °C (*green bars*); 24 h at 39.7 °C (*red bars*). For each virus, the amount of DNA accumulated during 24 h at 31.5 °C was defined as the maximum and set at 100%, and the other three values were expressed as a fraction of this value. For D*ts*27, only 0.7% of the maximal DNA levels had accumulated by 6 h at 31.5 °C,

which rose to 12% after 18 h at 39.7 °C. Thus, 11.3% of the maximum DNA levels were generated after shift-up to the non-permissive temperature, as opposed to the 0.1% of maximum DNA synthesized when the entire 24-h infection was performed at 39.7 °C (113-fold increase). These data suggest that allowing the initial 6 h of the D*ts*27 infection to proceed at the permissive temperature enables a marked, although incomplete, restoration of DNA synthesis. For D*ts*30, 3.4% of maximum DNA levels were synthesized after the shift to non-permissive temperature, which represented a 11-fold increase over the 0.3% levels of maximum DNA that accumulated when the full 24-h infection was performed at 39.7 °C. In this case, allowing the initial 6 h of D*ts*30 infections to proceed at the permissive temperature had a more modest impact on the restoration of DNA synthesis. For wt infections, equivalent amounts of DNA were synthesized whether the infections were shifted from permissive to non-permissive temperature or maintained exclusively at the non-permissive temperature (79 *versus* 74%).

*Cytoplasmic Extracts Prepared from Non-permissive Infections Lack Processive Polymerase Activity*—The DNA$^-$ phenotype seen during non-permissive D*ts*27 and D*ts*30 infections might have several mechanistic explanations. For example, defects in the E9 polymerase or the A20 protein compromise processive synthesis on a primed single-stranded template, whereas defects in the D5 NTPase or the B1 protein kinase do not (4, 6, 20). To determine whether the defect in UDG had an impact on processive DNA synthesis *per se*, we prepared cytoplasmic extracts from cells infected with *wt* virus, D*ts*27, or D*ts*30 at both the permissive and non-permissive temperatures. These extracts were tested for their ability to convert a singly-primed single-stranded M13 template into the double-stranded RFII form under conditions where the DNA polymerase itself is highly distributive. As shown in Fig. 2*A*, extracts prepared from *wt* infections maintained at both temperatures were competent for RFII formation. In contrast, the D*ts*27 extracts prepared at 31.5 °C retained RFII-forming activity, but those prepared at 39.7 °C did not. Extracts prepared from D*ts*30 infections performed at either temperature were unable to generate the RFII product. These data provide a correlation between the DNA$^-$ phenotype found *in vivo* with a lack of processive polymerase activity *in vitro* and implicate the D4 protein in the generation of the processive polymerase. When these extracts were assayed for the presence of distributive polymerase activity by measuring incorporation of [$\alpha$-$^{32}$P]dNTPs into an activated salmon sperm DNA template, comparable activity was found in all of the extracts (not shown). Immunoblot analyses of the extracts indicated that the A20 (and D5) proteins were present at *wt* levels within these extracts (Fig. 2*B*), indicating that the lack of processive polymerase activity was not an indirect effect of a loss of A20 stability or solubility. Due to the fact that we have been unsuccessful in developing an effective antibody against the vaccinia virus UDG, we could not perform immunoblot analysis to assess the stability of the *ts*UDG proteins.

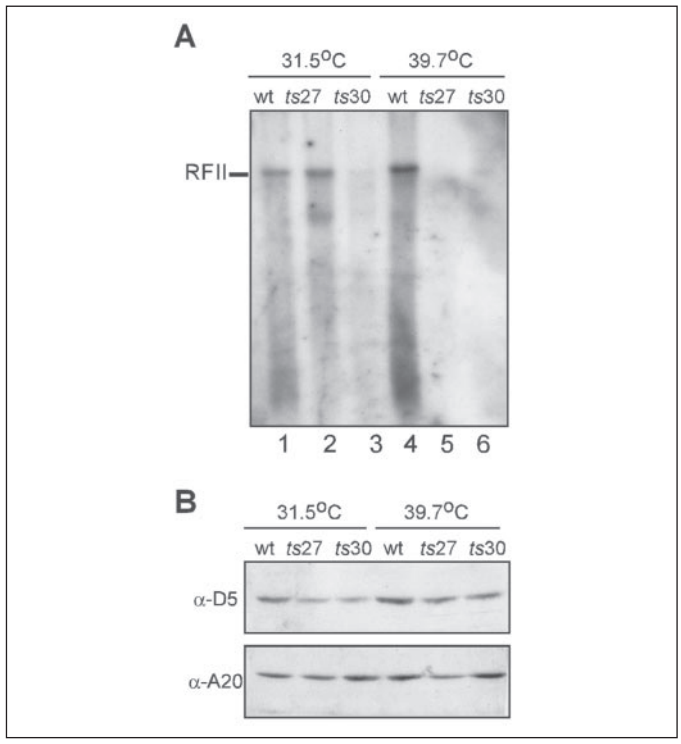


FIGURE 2. **Extracts prepared from non-permissive D*ts*27 and D*ts*30 infections do not direct processive DNA synthesis *in vitro*.** *A*, processive conversion of singly primed M13 template to ds RFII product. Confluent monolayers of BSC40 cells were infected with *wt* virus (WR strain) D*ts*27 or D*ts*30 (m.o.i. 15) and incubated at either 31.5 or 39.7 °C. Cytoplasmic extracts were prepared at 6 hpi, and aliquots were incubated with singly primed M13 DNA under standard reaction conditions described under "Experimental Procedures." An autoradiograph of the resolved products is shown; the RFII product is indicated. *B*, replication proteins A20 and D5 accumulate normally during *ts*D4 infections. BSC40 cells were infected with *wt* virus, D*ts*27 or D*ts*30 (m.o.i. 10) and maintained at 31.5 or 39.5 °C. At 8 hpi, cells were harvested and lysates were subjected to immunoblot analysis using antisera directed against A20 and D5.

### *Analysis of tsUDG/wt-A20 and tsA20/wt-UDG Interactions in Vitro*

Because both the D4 and A20 proteins appeared to be important in generating polymerase processivity (5, 6) and because a physical interaction between the two proteins had been previously demonstrated (11, 12), we hypothesized that the amino acid substitutions within the D4 proteins encoded by D*ts*27 and D*ts*30 might compromise this protein-protein interaction. To enable the direct analysis of the UDG-A20 interaction, we turned to coupled *in vitro* transcription-translation reactions (IVTT). First, we prepared a vector enabling the robust expression of N′-3×FLAG-tagged UDG (designated fUDG). Next, we generated a similar vector enabling the expression of a catalytically inactive version of fUDG (D68N and H181L; designated here as fUDG⃠ which has been shown to support virus viability in tissue culture (7). The comparable vector enabling the expression of untagged wt A20 was already in hand (6).

*A20-fUDG Interaction Is Preserved in Vitro and Does Not Require a Catalytically Active fUDG Enzyme*—IVTT reactions were programmed to express fUDG and/or wtA20, and translated reaction products were then subjected to affinity purification on $\alpha$-FLAG agarose beads. As shown in Fig. 3*A*, stoichiometric amounts of A20 were found to co-purify with fUDG (*lane 1*); this interaction was specific as A20 was not retrieved in the absence of fUDG (*lane 2*). If this assay is measuring an interaction that is important for viral DNA replication *in vivo*, then one would presume that the interaction would be retained in mixtures of fUDG⃠: plus *wt* A20. Indeed, this was the case, as seen in *lane 4*.

*ts30fUDG and tsA20-ER5 Show a Defect in Protein-Protein Interaction*—Similar vectors were therefore prepared for the D*ts*27 and D*ts*30 UDG alleles; in parallel, we also analyzed two previously prepared plasmids that directed the expression of the A20 proteins encoded by two *ts*A20 mutants (A20-6 and A20-ER5) (6). Individual IVTT reactions were programmed to express *wt* fUDG, *ts*27fUDG, *ts*30fUDG, *wt*A20, *ts*A20-5ER, and *ts*A20-6. Individual reactions and appropriate mixtures were then subjected to affinity purification on $\alpha$-FLAG-agarose beads. Care was taken to ensure that equivalent levels of each protein were present in each sample. Representative data are shown in Fig. 3*B*; as expected, significant levels of *wt*A20 were retrieved on the $\alpha$-FLAG-agarose beads in the presence, but not the absence, of *wt* fUDG (compare *lanes 3* with *1*). The degree of co-precipitation is expressed as the ratio of arbitrary units of A20: arbitrary units of fUDG. Similar levels of

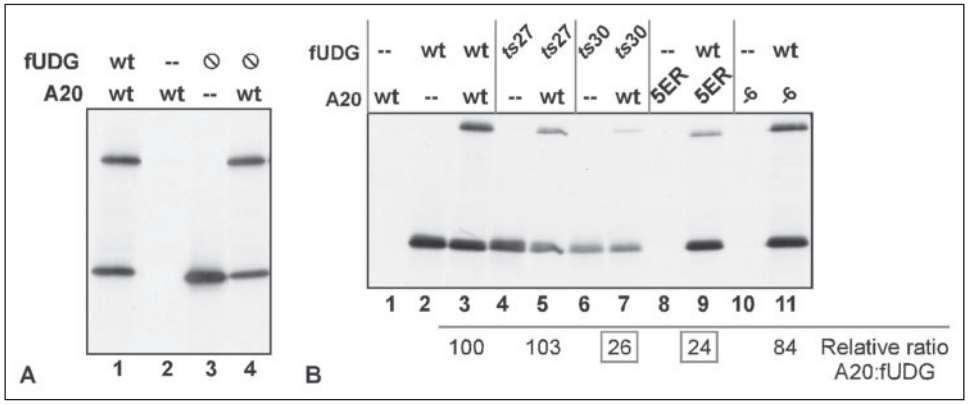


FIGURE 3. **The fUDG-A20 interaction is preserved *in vitro* and does not require a catalytically active UDG.** *A*, analysis of the interactions of fUDG and fUDG⊘ with A20 *in vitro*. A20 (*lanes 1*, *2*, and *4*) and fUDG (*lane 1*) or fUDG⊘ (catalytic null, *lanes 3* and *4*) were co-expressed in coupled *in vitro* transcription-translation (IVTT) reactions in the presence of [$^{35}$S]Met. Reactions were then subjected to affinity purification on α-FLAG-agarose beads, and the total reactions (not shown) and immunoprecipitates were fractionated on SDS-PAGE and visualized by autoradiography. *B*, analysis of tsUDG-wtA20 and tsA20-wtUDG interactions *in vitro*. Separate IVTT reactions were performed to express *wt* (*lanes 1*, *3*, *5*, and *7*) and mutant alleles of A20 (*lanes 8* and *9* for *ts*A20-5ER; *lanes 10* and *11* for *ts*A20-6) and *wt* (*lanes 2*, *3*, *9*, and *11*) and mutant alleles of fUDG (*ts*27, *lanes 4* and *5*; *ts*30, *lanes 6* and *7*). Translation products were then mixed appropriately and subjected to immunoprecipitation using α-FLAG-agarose beads. Aliquots of the immunoprecipitates were fractionated on SDS-PAGE, visualized by autoradiography, and quantitated by PhosphorImager analysis; the ratio of A20-fUDG for each *wt* and mutant pair was calculated and normalized to that seen for *wt*A20 plus wtfUDG (*lane 3*); relative ratios are shown beneath the appropriate lanes.

interaction were observed for mixtures of *ts*27fUDG plus *wt*A20 (*lane 5*) and *wt* fUDG plus *ts*A20-6 (*lane 11*). However, diminished interaction was consistently observed for mixtures containing *ts*30fUDG plus *wt*A20 (*lane 7*) and *wt* fUDG plus *ts*A20-5ER (*lane 9*). These data suggest that a defect in the UDG-A20 interaction might account for the DNA$^-$ phenotype and the absence of processive polymerase activity observed for D*ts*30 and *ts*A20-5ER.

### *Analysis of UDG in Vivo*

*Temporal Profile and Protein-Protein Interactions*—Analysis of the D4 protein *in vivo* has been hampered by the inability of our group and others to generate an effective anti-UDG antibody. Therefore, we generated a virus in which the endogenous D4 locus was replaced with one encoding N′-3×FLAG-tagged UDG (vvfUDG). This virus was indistinguishable from *wt* virus in terms of the yield produced during a single infectious cycle and the size of the plaques formed on BSC40 cells (not shown). Using this virus, we confirmed that UDG is expressed as an early protein, because immunoblot analyses with α-FLAG antiserum indicated that maximum levels of protein had accumulated by 4 hpi (Fig. 4*A*, *lanes 1*, *2*, and *4*). Moreover, accumulation was not hampered by the inclusion of 20 μM araC, an inhibitor of DNA synthesis and hence of intermediate and late gene expression, in the culture medium (*lane 3*).

*fUDG and A20 Interact When Expressed from Their Endogenous Loci*—To investigate whether endogenous fUDG and A20 interact during infection, cells were left uninfected or infected with *wt* virus or vvfUDG (m.o.i. 15). Cytoplasmic lysates were prepared at 2, 4, and 8 hpi and subjected to immunoprecipitation with α-A20 serum; immunoprecipitates were then subjected to immunoblot analysis with α-FLAG serum. As shown in Fig. 4*B*, fUDG co-immunoprecipitates with A20 when both are expressed at endogenous levels (*lanes 3–5*). This is the first evidence of their interaction *in vivo*.

### *Generation of vT7fUDG: Overexpression of fUDG within Vaccinia Virus-infected Cells*

Although vvfUDG was useful in our initial characterization of endogenously expressed FLAG-tagged UDG and its *in vivo* association with A20, we were unable to use this virus as a means of purifying fUDG to the levels required for further biochemical analyses. We therefore generated a recombinant virus encoding a copy of the fUDG gene under the regulation of a bacteriophage T7 promoter and encephalomyocarditis

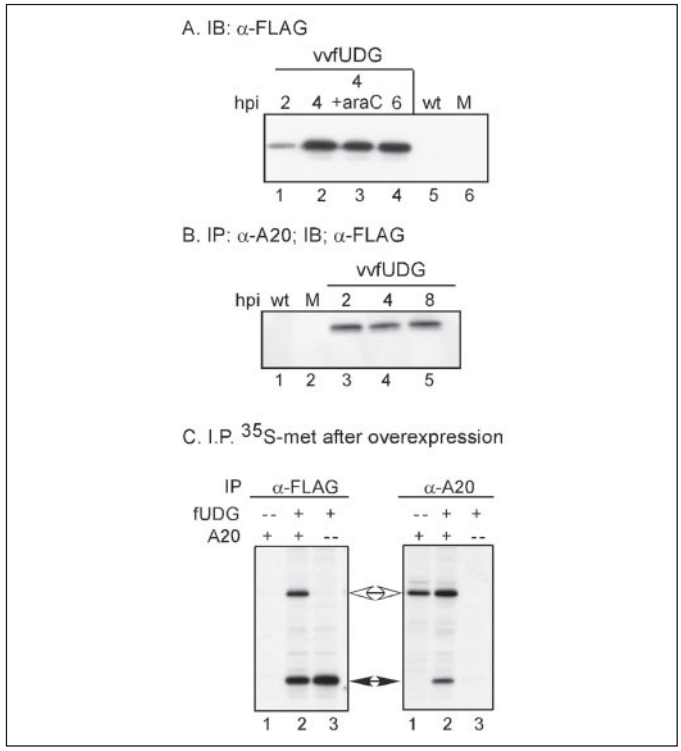


FIGURE 4. **Vaccinia virus UDG is an early protein that interacts with A20 *in vivo*.** *A*, UDG is expressed as an early protein. BSC40 cells were either mock infected (*lane 6*, *M*) or infected with a virus that expresses N′ 3×-FLAG-tagged UDG (vvfUDG) from the endogenous D4 locus (*lanes 1–4*) or with *wt* virus (*lane 5*) (m.o.i. 15). The DNA synthesis inhibitor araC (20 μM) was included where indicated (*lane 3*). Cytoplasmic lysates were prepared at 2, 4, and 6 hpi and subjected to immunoblot analysis with α-FLAG antibody. *B*, co-immunoprecipitation of endogenously expressed A20 and fUDG. BSC40 cells were either mock infected (*lane 2*, *M*) or infected with *wt* virus (*lane 1*) or vvfUDG (*lanes 3–5*) (m.o.i. 15). Cytoplasmic lysates were prepared at the times indicated (hpi) and subjected to immunoprecipitation with α-A20 antiserum; immunoprecipitates were resolved electrophoretically and subjected to immunoblot analysis with α-FLAG antibody. *C*, reciprocal co-immunoprecipitation of overexpressed fUDG and A20. BSC40 cells were infected (see "Experimental Procedures") so as to overexpress A20 (*lanes 1*), fUDG (*lanes 3*), or both (*lanes 2*); [$^{35}$S]Met was included in the culture medium from 6.5–8.5 hpi, at which point lysates were prepared and subjected to immunoprecipitation with sera directed against α-A20 (*right panel*) or α-FLAG (*left panel*). Immune complexes were resolved by SDS-PAGE and analyzed by fluorography. Radiolabeled species corresponding to fUDG (*lower*, *filled arrow*) and A20 (*upper*, *empty arrow*) are indicated.

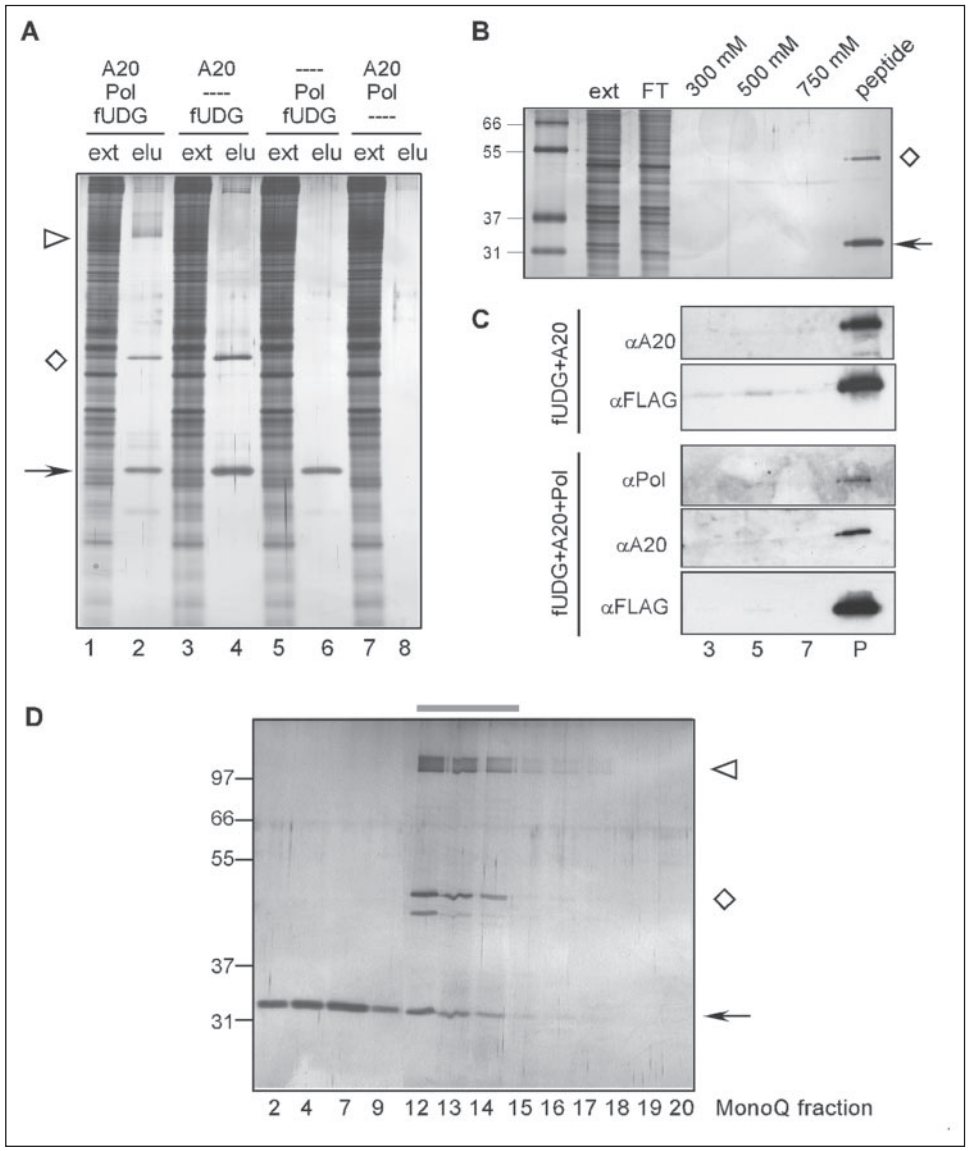


FIGURE 5. **Purification of stable complexes of fUDG-A20 and fUDG-A20-Pol.** *A*, BSC40 cells were infected appropriately to overexpress combinations of A20-E9 pol-fUDG, as indicated above the lanes. Cytoplasmic lysates were prepared at 24 hpi and incubated with α-FLAG-agarose beads; bound proteins were eluted by the addition of excess FLAG peptide. Aliquots of the extracts (*ext*, *lanes 1*, *3*, *5*, and *7*) and of the affinity purified eluates (*elu*, *lanes 2*, *4*, *6*, and *8*) were analyzed by SDS-PAGE followed by silver staining. The *arrow* indicates fUDG, the *diamond* indicates A20, and the *triangle* indicates the E9 DNA polymerase (*Pol*). (The higher molecular mass band (~200 kDa) in the eluates in *lanes 2*, *4*, and *8* is believed to be a nonspecific by-product of overexpression.) *B* and *C*, the fUDG-A20 and fUDG-A20-pol complexes are stable at high NaCl concentrations. BSC40 cells were infected to induce overexpression of fUDG-A20 or fUDG-A20-pol, and lysates were incubated with α-FLAG beads. The resin was then washed sequentially with buffer containing increasing concentrations of NaCl (300, 500, and 750 mM) and finally with an excess of the FLAG peptide. Aliquots of each elution were resolved by 12%-SDS-PAGE and subjected to silver staining (*B*) or immunoblot analysis with antisera directed against A20 or the FLAG epitope (*C*). *D*, further purification of the fUDG-A20-pol complex by Mono Q chromatography. The affinity-purified fUDG-A20-pol complex was applied to a Mono Q column, which was developed with a gradient of 150 mM to 1 M NaCl. Aliquots of each fraction were analyzed by SDS-PAGE and silver staining. The *gray bar* indicates the peak of the fUDG-A20-pol complex (fractions 12–14); free fUDG eluted in earlier fractions. The *arrow* indicates fUDG, the *diamond* indicates A20, and the *triangle* indicates the E9 DNA polymerase (*Pol*).

virus-untranslated leader (vTMfUDG). Overexpression of fUDG is induced upon co-infection with a virus encoding the T7 RNA polymerase (vTF7.5); comparable viruses enabling the overexpression of the E9 polymerase and the A20 protein have previously been generated in our laboratory (5, 14). The availability of these viruses enabled the overexpression of fUDG alone or in combination with A20 and/or the DNA polymerase.

*Co-immunoprecipitation of Overexpressed fUDG and A20*—The *in vivo* interaction between fUDG and A20 was confirmed by looking for their co-immunoprecipitation under conditions where both were overexpressed. Cells were infected with vT7A20, vT7fUDG, and vTF7.5 and metabolically labeled with [$^{35}$S]methionine from 6.5 to 8.5 hpi; lysates were subjected to immunoprecipitation analysis with α-A20 or α-FLAG sera (Fig. 4*C*). The radiolabeling of endogenous A20 and UDG is not significant in this experiment as both are early proteins and their synthesis declines after ~4 hpi. When fUDG was overexpressed alone, it was retrieved by the α-FLAG, but not the α-A20, serum (*lanes 3*). When A20 was overexpressed alone, it was retrieved by the α-A20, but not the α-FLAG, serum (*lanes 1*). When both proteins were overexpressed, we observed the reciprocal coprecipitation of fUDG and A20 by both sera (*lanes 2*). These results further support the conclusion that a substantial fraction of fUDG and A20 interact stably *in vivo*.

*A Stoichiometric Trimeric Complex of fUDG, A20, and the DNA Polymerase (E9) Is Purified When All Three Are Overexpressed in Vivo*—Based on the interaction between UDG and A20, and the previously demonstrated interaction between A20 and the E9 DNA pol (5), we hypothesized that the three proteins might interact to form a processive polymerase holoenzyme. We therefore used the hybrid vaccinia/T7 system to achieve the overexpression of fUDG and A20, fUDG and pol, fUDG, A20, and pol, or A20 and pol. Cells were harvested at 24 hpi, and clarified lysates were incubated with α-FLAG-agarose to purify fUDG and any interacting proteins. Bound proteins were eluted from the washed resin with competitor FLAG peptide and analyzed by SDS-PAGE. Fig. 5*A* shows the silver-stained profile of the soluble extracts (ext) and eluates (elu). When fUDG and A20 were overexpressed, they were retrieved in what appeared to be a stoichiometric dimeric complex (*lane 4*); ~2 μg of each protein was purified from $10^7$ cells. When fUDG, A20, and the DNA polymerase were overexpressed, the eluate contained all three proteins (*lane 2*). When fUDG and pol were overexpressed, pol was not co-purified with fUDG (*lane 6*). Because pol was only retrieved when A20 was also overexpressed, we concluded that there is a

"hierarchy" of binding and that E9 and fUDG do not interact directly. As expected, no proteins were retrieved when only A20 and pol were overexpressed (*lane 8*), because neither of these proteins contains a FLAG tag.

To assess the integrity and stability of the dimeric and trimeric protein complexes purified by affinity chromatography on α-FLAG-agarose, we took two approaches. First, we modified the purification profile by washing the resin with buffer containing 300, 500, and 750 mM NaCl prior to elution with FLAG peptide. The washes and the elutions were then resolved electrophoretically and analyzed by silver staining (Fig. 5*B*) and immunoblot analysis (Fig. 5*C*). As shown in 5*B*, which represents the purification of the dimeric A20-fUDG complex, the salt washes did not remove the bound A20, which remained on the column and was released with the fUDG upon the addition of FLAG peptide. The same result is seen in the *upper two blots* of *panel C*. When the trimeric complex of fUDG-A20-pol was similarly analyzed, we also saw that the vast majority of the A20 and pol proteins remained bound until the addition of peptide (*lower blots*). From these data we conclude that the A20-fUDG and A20-fUDG-pol complexes are quite stable.

The second approach taken to assess the integrity and stoichiometry of the complex was to apply the eluted fUDG-A20-pol complex to a Mono Q column and to monitor the chromatographic elution of the three proteins after development of the column with a gradient of 150 to 1000 mM NaCl. As shown in Fig. 5*D*, free fUDG eluted from the column in the early fractions (150–300 mM NaCl); in addition, we observed a second peak of protein (fractions 12–14, 540–590 mM NaCl), which contained fUDG-A20-pol. Fractions 12–14 were pooled, diluted, and applied to a second Mono Q column, which was developed in the same manner; again, the three proteins eluted together in fractions 12–14 (550–590 mM NaCl (not shown)). Cumulatively, these data confirm that fUDG, A20, and pol associate in a heterotrimeric complex and that this complex has an approximate stoichiometry of 1:1:1.

*fUDG-A20-pol Complex Is Necessary and Sufficient for Processive Polymerase Activity*—We have previously used the conversion of a singly primed M13 template to the fully replicated RFII form as an assay for processive DNA synthesis (21). In this manner, it was determined that processive synthesis requires both the DNA polymerase (E9) and other early viral protein(s) (20), one of which was purified and identified as the product of the A20R gene (5). It is reasonable to hypothesize that UDG might be a second component of the processivity factor.

The extracts and eluates prepared from cells induced to overexpress various combinations of fUDG, A20, and pol were therefore assayed for their ability to direct processive synthesis on the same singly primed M13 template that we have used previously to study purified polymerase, cytoplasmic extracts, and enriched preparations of the processive polymerase (4, 5, 20). These data are shown in Fig. 6*A*; the extracts are shown in the *odd lanes* (*1*, *3*, *5*, *7*, and *9*) and the corresponding eluates in the *even lanes* (*2*, *4*, *6*, *8*, and *10*). The extract containing overexpressed fUDG alone had a low level of RFII-forming activity that was set as 1; the activity of the other extracts was normalized to this level. We quantitated both the full range of products present in the entire lane as well as the level of full-length RFII. Overexpression of fUDG and pol raised the total product level 5-fold and the level of RFII product 3.8-fold, whereas overexpression of A20 and fUDG or A20 and pol raised the total level of product 10-fold and the levels of RFII product 22- and 25-fold, respectively. Of note, however, is the observation that overexpression of fUDG, A20, and pol increased the total product 24-fold and the level of RFII product 88-fold. It is important to note that the impact of fUDG and A20 on the level of synthesis seen in these reactions is due to a gain in processivity rather than an intrinsic stimulation of catalytic activity, because extracts containing either overexpressed pol or overexpressed pol-A20 and/or fUDG had comparable levels of distributive polymerase activity as assayed on an activated salmon-sperm template (not shown).

Analysis of the eluates was even more informative. No detectable activity could be measured in the eluate from fUDG-overexpressing extracts (which contains fUDG) or from the A20-pol extracts (which contains no detectable proteins). A low level of activity was retrieved from the fUDG-pol-overexpressing extracts; this value was set to 1 and used as the baseline for normalization of the other eluates. The eluate retrieved from the fUDG-A20-overexpressing extracts showed a 7.4-fold increase in the level of total product formed and a 56-fold increase in the level of RFII product formed. This eluate contains some endogenous pol, which associates with the overexpressed proteins. Most importantly, the eluate retrieved from the fUDG-A20-pol extracts was 56-fold more active in the synthesis of total products, and 740-fold more active in the synthesis of full-length RFII product. This eluate was further subjected to a time course assay, to confirm that the rate of RFII formation was comparable to that which we had observed earlier for the processive polymerase activity found in infected cell extracts (20). As shown in Fig. 6*B*, the fUDG-A20-pol complex could indeed form complete RFII product after 5 min of reaction, with the amount of full-length product increasing thereafter.

Because fUDG appears to interact directly with A20 (but not with Pol), and because A20 appears to interact directly with pol, we attempted to reconstitute processive pol activity by mixing the fUDG-A20 eluate with purified pol protein. This pol protein was purified by conventional chromatography (14); its enzymatic activity is highly distributive under the assay conditions used here (20). The results of such an experiment are shown in Fig. 6*C*. As shown previously, the RFII-forming activity of extracts (*lanes 1* and *3*) and eluates (*lanes 2* and *4*) prepared from cells overexpressing only fUDG-A20 is significantly lower than that retrieved from cells overexpressing fUDG-A20-pol. Indeed, the eluate from the fUDG-A20 extract has only a trace level of activity (*lane 4*). However, addition of 1.5 ng of purified pol to this eluate restored a robust level of processive polymerase activity (*lane 5*); we estimate that 1.5 ng of pol is roughly equivalent to the amount of pol present in the aliquot of eluate assayed in *lane 2*. In contrast, no RFII was formed when 5 ng of the pol prep was assayed on its own (*lane 6*).

These data provide compelling evidence that fUDG, A20, and pol are necessary for assembly of a processive polymerase holoenzyme. To reinforce the conclusion that they are sufficient, we took advantage of two further preparations described above. First, we took advantage of the fact that fUDG, A20, and pol remain bound to the α-FLAG matrix in the presence of 750 mM NaCl and are only released upon the addition of FLAG peptide. This eluate, which should be free of contaminating proteins that are not an intrinsic part of the complex, was also monitored for its processive polymerase activity in the RFII-forming assay. As shown in Fig. 6*D*, the eluate prepared in this way retained robust RFII-forming activity (*lane 6*); if anything, the specific activity of this final eluate was higher than that obtained from peptide elutions performed without prior high salt washes.

Secondly, as described above, the fUDG-A20-pol complex retrieved by affinity chromatography can be resolved from free fUDG, and presumably from other contaminants, by chromatography on Mono Q (Fig. 5*D*). Fractions from this chromatographic separation were also assayed for RFII-forming activity (Fig. 6*E*). A peak of enzymatic activity was seen in Fractions 12–14, which corresponds with the elution of fUDG, A20, and pol (Fig. 5*D*).

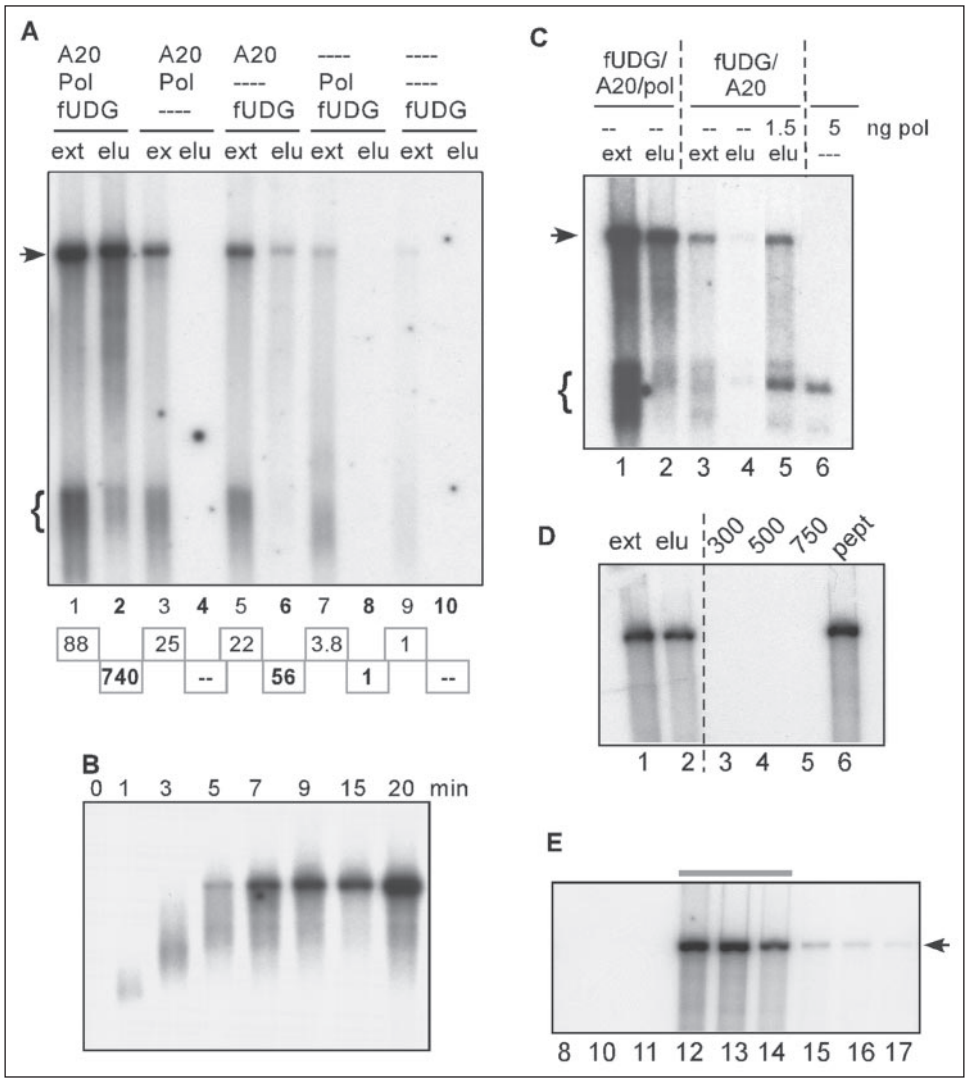


FIGURE 6. **The fUDG-A20-Pol complex has processive polymerase activity.** *A*, assay of extracts and eluates for their ability to form the RFII product in a processive manner. BSC40 cells were infected so as to overexpress fUDG, A20, and pol in various combinations as indicated above the lanes. At 24 hpi, extracts were prepared and incubated with α-FLAG beads; bound proteins were eluted with FLAG peptide. The extracts (*ext*, *odd-numbered lanes*) and eluates (*elu*, *even-numbered lanes*, in *bold*) were then evaluated for their ability to complete RFII formation on a singly primed M13 template. An autoradiograph of the resolved products is shown. The levels of full-length RFII product generated by the extracts were normalized to that produced by the extract containing overexpressed fUDG; these relative values are shown as *boxed numbers* below the *odd-numbered lanes*. The levels of RFII product generated by the eluates were normalized to that produced by the eluate containing fUDG alone; these relative values are shown as *boxed numbers* below the *even-numbered lanes*. The *bracket* indicates the short DNA products generated by distributive synthesis. *B*, the fUDG-A20-pol complex completes RFII synthesis in 5 min. Multiple replication reactions containing the purified fUDG-A20-pol complex were performed in parallel; individual reactions were quenched at the indicated times after the initiation of primer elongation. An autoradiograph of the resolved products is shown. *C*, the fUDG-A20 complex is sufficient to confer processivity on the E9 polymerase. Extracts or affinity purified eluates prepared from cells infected so as to overexpress the indicated viral proteins were assayed for their ability to perform processive synthesis and generate RFII products. *Lane 5* contains a reaction comparable to that shown in *lane 4* except for the addition of 1.5 ng of purified E9 pol. A control reaction containing 5 ng of purified pol (without any extract or eluate) was also performed (*lane 6*). The *arrow* indicates the RFII product; the *bracket* indicates the short products formed by distributive synthesis. *D*, the RFII-forming activity of the fUDG-A20-pol complex is not diminished by prior washes with high concentrations of NaCl. Extracts prepared from cells infected so as to overexpress fUDG-A20-pol were prepared, applied to α-FLAG-agarose, and either eluted directly with FLAG peptide (*lane 2*), or first subjected to sequential washes with buffer containing the indicated concentrations of NaCl (*lanes 3–5*) prior to peptide elution (*pept*, *lane 6*). Each sample was then assayed for its ability to perform processive DNA synthesis and generate RFII products. *E*, the fUDG-A20-pol complex retains RFII-forming activity after further purification by Mono Q chromatography. The affinity purified fUDG-A20-pol complex was resolved from free fUDG by chromatography on Mono Q-Sepharose as shown in Fig. 5*D*. The *gray bar* indicates fractions 12–14; these fractions contain the eluted fUDG-A20-pol complex (see Fig. 5*D*) and have robust RFII-forming activity.

In sum, these data provide strong evidence for the hypothesis that fUDG, A20, and pol are necessary and sufficient for the generation of a processive DNA polymerase holoenzyme.

*Contribution of fUDG to Processive Polymerase Activity Is Independent of Residues That Contribute to Uracil Binding or Catalysis*—The UDG encoded by vaccinia virus must play several roles in the infectious cycle. The virus cannot replicate at all without expression of UDG (10), but an allele that encodes a stable but catalytically inert protein will sustain full replication in tissue culture (7). Viruses bearing this allele are attenuated in mice, however (7). We would presume that the essential role of UDG in generating the processive polymerase holoenzyme is independent of its catalytic activities. In mice, however, the ability of UDG to recognize dUMP moieties within the genome, and to initiate their excision and repair, must be essential. To test this prediction, we examined two mutant forms of fUDG for their ability to form a proficient fUDG-A20-pol complex. First, we utilized the previously described UDG allele (D68N and H181L; fUDG⍉), which encodes a protein that lacks catalytic activity but sustains vaccinia replication in tissue culture (7). As shown in Fig. 7*A*, complexes of fUDG⍉-A20-pol show the same level of processive polymerase activity as do *wt* com-

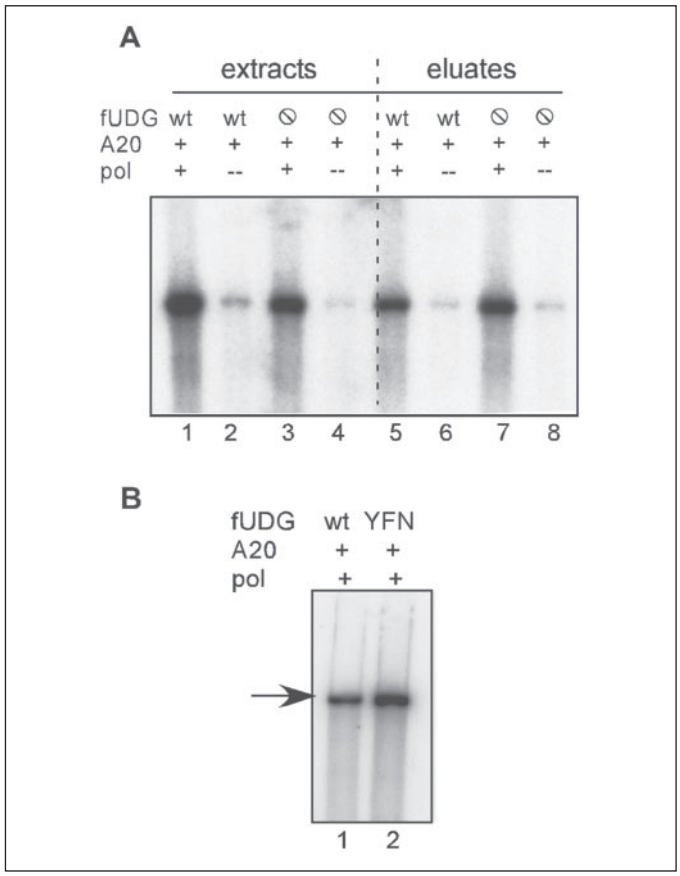


FIGURE 7. **The contribution of the UDG protein to the formation of the processive polymerase is independent of amino acids implicated in uracil recognition or catalysis.** *A*, cells were infected so as to overexpress A20 and either *wt* or catalytically inactive fUDG (⊘), with or without the simultaneous overexpression of E9 pol, as indicated. Extracts (*lanes 1–4*) and affinity-purified eluates (*lanes 5–8*) were assayed for their ability to direct processive synthesis and generate RFII product. An autoradiograph of the resolved products is shown. *B*, BSC40 cells were infected so as to overexpress A20, E9 pol, and either *wt* fUDG or fUDG-YFN (⊗). Following affinity purification on α-FLAG-agarose beads, the eluates were evaluated for their ability to complete processive synthesis. An autoradiograph of the resolved products is shown; the RFII product is indicated by the *arrow*.

plexes prepared in parallel (*e.g.* compare *lanes 1* with *3* and *5* with *7*). Second, we generated an allele containing Y70A, F79A, and N120A substitutions, which should disrupt the ability of UDG to recognize and pause at incorporated dUMP residues as it tracks along a DNA substrate (fUDG-YFN [⊗]) (22, 23). Complexes containing fUDG (wt or ⊗), A20, and pol were prepared by affinity purification. The protein composition was confirmed by SDS-PAGE and silver staining (not shown), and eluates were tested in parallel for RFII-forming activity. We observed that complexes of fUDG⊗-A20-pol possessed the same processive polymerase activity as did the complexes containing *wt* fUDG (Fig. 7*B*, compare *lanes 1* and *2*). From these data, we conclude that the role of UDG as an essential component of the processivity factor is independent of residues that confer the ability to recognize or excise uracil.

## DISCUSSION

In this report, we address the role of the vaccinia UDG in viral DNA replication. Initial evidence for the involvement of UDG in this process came from the observation that D*ts*30 (formerly known as *ts*4149), whose temperature sensitivity is due to a mutation in the D4R gene that encodes UDG, has a DNA$^-$ phenotype at the non-permissive temperature (24). Since then, the D4 protein has been shown to interact directly with the A20 protein (11, 12), which has been shown genetically and biochemically to be essential for DNA replication *in vivo* and to be a stoichiometric component of the processive DNA polymerase complex (5, 6, 25). Most recently, a virus lacking the D4R gene has been generated; this virus, which is propagated in a complementing cell line, has provided direct confirmation that viral DNA replication is abrogated in the absence of UDG expression (7). The studies presented here extend and unite these observations by providing compelling evidence that a complex of A20 and D4 functions as the processivity factor for the vaccinia DNA polymerase.

To facilitate an analysis of UDG *in vivo*, we generated a virus in which the endogenous D4 allele now encodes a 3×FLAG-tagged version of D4. Using this virus, we were able to demonstrate that the epitope-tagged protein supports virus viability and that D4 and A20 interact *in vivo*. By metabolically labeling cultures with [$^{35}$S]Met or [$^{32}$P]$P_i$, we confirmed that D4 is expressed as an early protein but were unable to detect any phosphorylation of UDG. We also studied infections performed with both D*ts*30 and D*ts*27, which map to the same complementation group (26). We determined that D*ts*27 encodes a UDG protein bearing a Leu$^{110}$ → Phe substitution. D*ts*27 has a classic *ts* phenotype, producing *wt* levels of virus at 31.5 °C and 1000-fold less infectious virus at 39.7 °C; similarly, DNA synthesis proceeded to *wt* levels at 31.5 °C and was essentially blocked at 39.7 °C. Moreover, extracts prepared from 31.5 °C infections were active in replicating a singly primed DNA substrate in a processive manner, whereas those prepared at 39.7 °C lacked this activity. D*ts*30 showed somewhat different characteristics, being partially impaired in both virus production and DNA replication at the permissive temperature. In keeping with this impairment, extracts prepared from cells infected with D*ts*30 at either permissive or non-permissive temperatures were unable to direct processive DNA synthesis *in vitro*. We also observed that, when interactions between D4 and A20 were examined in an assay involving co-immunoprecipitation of IVTT-synthesized proteins, D*ts*30-D4 showed a reduced ability to interact with A20.

Construction of recombinant vaccinia viruses that can be induced to overexpress fUDG (or a catalytically null variant, fUDG⊘) enabled us to investigate the interactions between D4, A20, and the E9 Polymerase. We determined that fUDG interacts directly with A20 forming a dimeric complex and that fUDG-A20 together can associate with the E9 DNA pol in a trimeric complex. Both the dimeric and trimeric complexes remained intact in the presence of 750 mM NaCl, and both could be further purified by chromatography on sequential Mono Q columns, indicating that the complexes are highly stable. The catalytic activity of UDG was not important for interaction with A20, as might have been expected by the viability of a virus encoding only a catalytically null variant of UDG (7).

Retrieval of these complexes enabled us to examine whether these three proteins were necessary and sufficient for the assembly of a processive DNA polymerase. Indeed, the trimeric complex of fUDG-A20-pol had robust processive synthesis activity, which was not diminished by prior washes of 750 mM NaCl or by chromatography on a Mono Q anion exchange column. Moreover, addition of purified E9 pol to the fUDG-A20 complex restored processive synthesis activity. Taken together, these data provide strong evidence that the three proteins comprise the polymerase holoenzyme.

The interaction of fUDG and A20 can be readily recapitulated with proteins synthesized by IVTT. In contrast, we have been unable to demonstrate any interaction between IVTT-synthesized pol and IVTT-synthesized A20 and/or A20-UDG. We considered two explanations for this result: (i) either a fourth viral or cellular protein is required to mediate the initial association of pol with the complex or (ii) pol and/or

A20-UDG undergo post-translational modifications *in vivo* that facilitate complex formation. To date, we have no evidence that any additional proteins are consistently retrieved in our affinity-purified complexes, and our attempts to detect any phosphorylation of pol, A20, or UDG *in vivo* have been negative. Clarification of what factor(s) currently limit the reconstitution of the holoenzyme from proteins synthesized exclusively *in vitro* will be addressed in future studies.

We believe that UDG and A20 are constitutively associated; based on silver stain analysis of preparations of affinity-purified samples further subjected to Mono Q chromatography or glycerol gradient analysis (not shown), we believe that they form a heterodimer. Previously, we have experienced great difficulty in producing soluble A20 protein in any system designed for the production of recombinant proteins; however, A20 is soluble and easily studied when it is co-expressed with UDG. We believe that the proper folding of A20 is dependent upon its association with UDG. The Moss laboratory has demonstrated that the N′ 25 amino acids of A20 contain the minimal binding site for the UDG protein, although amino acids 25–50 increase the efficiency of this reaction (11). We believe that A20 serves as a bridge between UDG and the DNA polymerase, because these two proteins do not appear to interact directly. A20 may also serve as a scaffold that brings other replication factors with which it interacts, such as D5, to the replication fork. A20 may also provide a bridge between replicating genomes and proteins, such as its third binding partner H5, that may serve as an organizing substratum on which replication occurs.

Most, if not all, replicative polymerases are intrinsically distributive. They rely on processivity factors to facilitate the rapid duplication of long DNA molecules. The challenge for such factors is the requirement to tether the polymerase to the DNA template without impeding its rapid translocation. One elegant solution to this problem is exemplified by the processivity factors associated with cellular DNA polymerases, which function as toroidal sliding clamps. For example, a dimer of the $\beta$-subunit of *E. coli* (27, 28) and a trimer of the eukaryotic PCNA protein (29, 30) are loaded onto DNA by ATP-dependent clamp loaders (reviewed in Refs. 31 and 32). These processivity factors, which encircle but do not bind to DNA, interact with their cognate polymerases and so tether them to the DNA in a manner that allows rapid translocation (reviewed in Ref. 33). The processivity factor of the bacteriophage T4 belongs to this same class of proteins (34, 35), but other viral processivity factors have distinct modes of action. In bacteriophage T7, thioredoxin forms a 1:1 complex with the polymerase without any need for a clamp loader (36); the mechanism by which thioredoxin confers processivity remains poorly understood. The polymerases encoded by diverse human herpesviruses also associate with processivity factors in the absence of a clamp loader; these processivity factors are represented by the UL42 protein of herpes simplex virus I, the BMRF1 protein of Epstein-Barr virus, a dimer of the UL44 protein in human cytomegalovirus (CMV), and a dimer of the PF-8 protein in Kaposi's sarcoma virus.

The structure and function of the UL42 protein have been studied extensively; during strand elongation, UL42 translocates with the catalytic subunit of the polymerase by linear diffusion, despite the fact that it demonstrates high affinity for DNA (37). In fact, the UL42 protein will remain on the DNA until it can slide off a free end (37). Moreover, UL42 appears to facilitate the loading of the polymerase onto DNA, to increase the preference of polymerase for binding to primer/template junctions, and to slow the dissociation of polymerase from DNA without reducing its elongation rate (38, 39). Amino acid substitutions on the basic surface of the UL42 protein, which specifically disrupt DNA binding, negatively affect processivity (40). Thus, the DNA binding properties of UL42 are central for its role in processivity. Despite possessing a significantly different mode of action from the sliding clamp loaders such as PCNA, structural analysis of UL42 has shown that it contains a "processivity fold" that is highly reminiscent of PCNA (41). The processivity factor of CMV, UL44, also contains this "processivity fold." Interestingly, however, it functions as a C-shaped dimer that partially encircles the DNA as well as functioning as a direct DNA-binding protein (42). Thus, UL44 is considered to be a hybrid processivity factor. These in-depth studies of UL42 and UL44 will help to shape our future determinations of how UDG and/or A20 interact with the DNA template and confer processivity on the E9 polymerase.

In mammalian cells, the nuclear form of UDG (UNG2) interacts physically with both PCNA (processivity factor) and replication protein A (single-stranded DNA binding protein) in replication foci (43, 44). This association with the moving replication fork allows UDG to recognize and excise dUMP residues as they are misincorporated by the polymerase. The UDG encoded by CMV (UL114) has also been shown to associate with replication foci; moreover, deletion of UDG delays and diminishes replication (45, 46). In CMV, as in vaccinia, the uracil-removing function of UDG does not appear to be the important contribution to replication, as poor viral replication was unrelated to the uracil content of input genomes (46). Thus, there is precedent for the involvement of UDG in replication complexes, and it would appear that vaccinia virus has taken the concept of bringing UDG to the moving replication fork to a new level by utilizing it as a component of the processivity factor.

The identification of the UDG-A20 complex as the processivity factor for the vaccinia DNA polymerase opens new opportunities for understanding the mechanism by which processivity is acquired. Although UDG is generally thought of as a repair enzyme, a closer look at the mechanism these enzymes employ to scan the DNA in search of uracil residues reveals a process that would be favorable for a processivity factor. UDG enzymes appear to scan the DNA in a processive manner, binding, kinking, and compressing the DNA backbone as it looks for dUMP residues (22). This process has been characterized as employing a "pinch-push-pull" mechanism (22, 23). Once uracil is detected, the enzyme flips the base out of the DNA base stack and into the UDG active-site pocket, causing the DNA to bend further and the enzyme to encircle the extrahelical uracil and deoxyribose. The fact that this nucleotide flipping step occurs only at uracil residues would allow for rapid translocation along a non-uracil containing template DNA.

The vaccinia UDG has diverged significantly from the UDGs encoded by *E. coli*, humans, and herpes simplex virus I, although many of the residues known to be involved in uracil recognition and flipping, and catalytic activity, are preserved (7). A notable exception is $Leu^{272}$, which is not present in vaccinia. It is the side chain of this leucine residue that is thought to be inserted into the DNA minor groove as part of "the minor groove reading head" (22, 23). Despite containing some substitutions in important motifs shared by the majority of UDG enzymes, the vaccinia UDG is known to effectively remove uracil residues from exogenous templates *in vitro* (9) and presumably *in vivo* as well. The Moss laboratory has shown that a catalytically null variant of UDG supports viral replication in tissue culture (7), and the studies described herein confirm that neither catalytic activity, nor residues associated with uracil recognition, are required for the function of UDG as a component of the processivity factor. Rather, we believe that the core function of UDG is to scan DNA in a processive manner; because UDG binds tightly to A20, and A20 to pol, processive synthesis is enabled. Further confirmation of this model, identification of the one or more domains of UDG that interact with the N′ terminus of A20, and dissection of the A20 and pol interaction, are subjects for future study. By extrapolating from

studies of the herpes simplex virus and CMV polymerase holoenzymes (37–39, 42, 47, 48), we would also propose that identification of small molecules that disrupt the A20-UDG interface represents a novel and effective strategy for the generation of anti-poxvirus compounds.

*Acknowledgments—We thank Mira Punjabi and Kathleen Boyle for providing helpful reagents and for their assistance and expertise.*

## REFERENCES


1. Garcia, A. D., Aravind, L., Koonin, E. V., and Moss, B. (2000) *Proc. Natl. Acad. Sci. U. S. A.* **97,** 8926–8931
2. Beaud, G. (1995) *Biochimie.* (*Paris*) **77,** 774–779
3. Traktman, P. (1996) *Poxvirus DNA replication. DNA Replication in Eukaryotic Cells* (De Pamphilis, ME, ed) pp. 775–798, Cold Spring Harbor Laboratory Press, Cold Spring Harbor, NY
4. McDonald, W. F., and Traktman, P. (1994) *J. Biol. Chem.* **269,** 31190–31197
5. Klemperer, N., McDonald, W., Boyle, K., Unger, B., and Traktman, P. (2001) *J. Virol.* **75,** 12298–12307
6. Punjabi, A., Boyle, K., DeMasi, J., Grubisha, O., Unger, B., Khanna, M., and Traktman, P. (2001) *J. Virol.* **75,** 12308–12318
7. De Silva, F. S., and Moss, B. (2003) *J. Virol.* **77,** 159–166
8. Millns, A. K., Carpenter, M. S., and DeLange, A. M. (1994) *Virology* **198,** 504–513
9. Upton, C., Stuart, D. T., and McFadden, G. (1993) *Proc. Natl. Acad. Sci. U. S. A.* **90,** 4518–4522
10. Stuart, D. T., Upton, C., Higman, M. A., Niles, E. G., and McFadden, G. (1993) *J. Virol.* **67,** 2503–2512
11. Ishii, K., and Moss, B. (2002) *Virology* **303,** 232–239
12. McCraith, S., Holtzman, T., Moss, B., and Fields, S. (2000) *Proc. Natl. Acad. Sci. U. S. A.* **97,** 4879–4884
13. Punjabi, A., and Traktman, P. (2005) *J. Virol.* **79,** 2171–2190
14. McDonald, W. F., and Traktman, P. (1994) *Protein Expr. Purif.* **5,** 409–421
15. Franke, C. A., Rice, C. M., Strauss, J. H., and Hruby, D. E. (1985) *Mol. Cell Biol.* **5,** 1918–1924
16. DeMasi, J., and Traktman, P. (2000) *J. Virol.* **74,** 2393–2405
17. Grubisha, O., and Traktman, P. (2003) *J. Virol.* **77,** 10929–10942
18. Evans, E., and Traktman, P. (1987) *J. Virol.* **61,** 3152–3162
19. McIntosh, A. A., and Smith, G. L. (1996) *J. Virol.* **70,** 272–281
20. McDonald, W. F., Klemperer, N., and Traktman, P. (1997) *Virology* **234,** 168–175
21. Traktman, P., and Boyle, K. (2004) *Methods Mol. Biol.* **269,** 169–186
22. Parikh, S. S., Mol, C. D., Slupphaug, G., Bharati, S., Krokan, H. E., and Tainer, J. A. (1998) *EMBO J.* **17,** 5214–5226
23. Parikh, S. S., Putnam, C. D., and Tainer, J. A. (2000) *Mutat. Res.* **460,** 183–199
24. McFadden, G., and Dales, S. (1980) *Virology* **103,** 68–79
25. Ishii, K., and Moss, B. (2001) *J. Virol.* **75,** 1656–1663
26. Lackner, C. A., D'Costa, S. M., Buck, C., and Condit, R. C. (2003) *Virology* **305,** 240–259
27. Stukenberg, P. T., Studwell-Vaughan, P. S., and O'Donnell, M. (1991) *J. Biol. Chem.* **266,** 11328–11334
28. Kong, X. P., Onrust, R., O'Donnell, M., and Kuriyan, J. (1992) *Cell* **69,** 425–437
29. McConnell, M., Miller, H., Mozzherin, D. J., Quamina, A., Tan, C. K., Downey, K. M., and Fisher, P. A. (1996) *Biochemistry* **35,** 8268–8274
30. Krishna, T. S., Kong, X. P., Gary, S., Burgers, P. M., and Kuriyan, J. (1994) *Cell* **79,** 1233–1243
31. Trakselis, M. A., and Benkovic, S. J. (2001) *Structure.* (*Camb.*) **9,** 999–1004
32. Kelman, Z., Hurwitz, J., and O'Donnell, M. (1998) *Structure* **6,** 121–125
33. Bruck, I., and O'Donnell, M. (2001) *Genome Biology* http://genomebiology.com/2001/2/1/reviews/3001
34. Moarefi, I., Jeruzalmi, D., Turner, J., O'Donnell, M., and Kuriyan, J. (2000) *J. Mol. Biol.* **296,** 1215–1223
35. Yao, N., Turner, J., Kelman, Z., Stukenberg, P. T., Dean, F., Shechter, D., Pan, Z. Q., Hurwitz, J., and O'Donnell, M. (1996) *Genes Cells* **1,** 101–113
36. Johnson, D. E., and Richardson, C. C. (2003) *J. Biol. Chem.* **278,** 23762–23772
37. Randell, J. C., and Coen, D. M. (2001) *Mol. Cell* **8,** 911–920
38. Trego, K. S., Zhu, Y., and Parris, D. S. (2005) *Nucleic Acids Res.* **33,** 536–545
39. Weisshart, K., Chow, C. S., and Coen, D. M. (1999) *J. Virol.* **73,** 55–66
40. Randell, J. C., Komazin, G., Jiang, C., Hwang, C. B., and Coen, D. M. (2005) *J. Virol.* **79,** 12025–12034
41. Zuccola, H. J., Filman, D. J., Coen, D. M., and Hogle, J. M. (2000) *Mol. Cell* **5,** 267–278
42. Appleton, B. A., Loregian, A., Filman, D. J., Coen, D. M., and Hogle, J. M. (2004) *Mol. Cell* **15,** 233–244
43. Akbari, M., Otterlei, M., Pena-Diaz, J., Aas, P. A., Kavli, B., Liabakk, N. B., Hagen, L., Imai, K., Durandy, A., Slupphaug, G., and Krokan, H. E. (2004) *Nucleic Acids Res.* **32,** 5486–5498
44. Otterlei, M., Warbrick, E., Nagelhus, T. A., Haug, T., Slupphaug, G., Akbari, M., Aas, P. A., Steinsbekk, K., Bakke, O., and Krokan, H. E. (1999) *EMBO J.* **18,** 3834–3844
45. Prichard, M. N., Duke, G. M., and Mocarski, E. S. (1996) *J. Virol.* **70,** 3018–3025
46. Prichard, M. N., Lawlor, H., Duke, G. M., Mo, C., Wang, Z., Dixon, M., Kemble, G., and Kern, E. R. (2005) *Virol. J.* **2,** 55
47. Chaudhuri, M., and Parris, D. S. (2002) *J. Virol.* **76,** 10270–10281
48. Thornton, K. E., Chaudhuri, M., Monahan, S. J., Grinstead, L. A., and Parris, D. S. (2000) *Virology* **275,** 373–390